Lanthanide and alkaline-earth complexes of EDTA in water: a molecular dynamics study of structures and binding selectivities †

Sylvie Durand,[a] Jean-Pierre Dognon,[a] Philippe Guilbaud,[a] Catherine Rabbe[a] and Georges Wipff*[b]

[a] *Laboratoire de Chimie Théorique et Structurale, Commissariat à l'Energie Atomique, CEA/Valrhô, Centre de Marcoule, BP 171, 30200 Bagnols-sur-Cèze, France*
[b] *Laboratoire de Modélisation et Simulations Moléculaires, Institut de Chimie, Université Louis Pasteur, 4 rue Blaise Pascal, 67000 Strasbourg, France*

Received (in Cambridge, UK) 8th November 1999, Accepted 7th December 1999

We report a molecular dynamics (MD) study on M^{3+} lanthanide and M^{2+} alkaline-earth complexes of ethylenediaminetetraacetate tetraanion ($EDTA^{4-}$) in aqueous solution. First, a consistent set of Lennard-Jones parameters for La^{3+}, Eu^{3+} and Lu^{3+} cations has been derived from MD and free energy calculations. It reproduces the experimental differences in their hydration free energies, lanthanide–water distances and coordination numbers in water. Next, the uncomplexed $EDTA^{4-}$ ligand has been simulated in the presence of Na^+, Ca^{2+} or Eu^{3+} neutralizing counterions, leading to the spontaneous complexation of Na^+, but not of Ca^{2+} or Eu^{3+} whose complexes are more stable. The *endo* 1 : 1 complexes of M^{2+} and M^{3+} cations, simulated for up to 1 ns, remain of inclusive type during the whole simulation. The calculated binding selectivities nicely reproduce experimental trends in relative stabilities with $EDTA^{4-}$ in each cation series: $Ca^{2+} > Sr^{2+} > Ba^{2+}$ and $Lu^{3+} > Eu^{3+} > La^{3+}$. Thus, despite the simplicity of the cation models (1–6–12 pairwise additive interactions without explicit polarization or charge transfer effects), structural and energy features of lanthanide and alkaline-earth complexation by polyaminocarboxylate ligands are, at least, qualitatively, accounted for.

Introduction

Polyaminocarboxylate ligands such as EDTA, TETA or DOTA form strong complexes with alkaline-earth, trivalent lanthanides or actinides in aqueous solution,[1–4] which may be of interest in the context of An(III)/Ln(III) separation processes.[5–7] In this paper, we report molecular dynamics (MD) simulations on the complexation of typical alkaline-earth (Ca^{2+}, Sr^{2+} and Ba^{2+}) and lanthanide (La^{3+}, Eu^{3+} and Lu^{3+}) cations by the ethylenediaminetetraacetate $EDTA^{4-}$ tetraanion ligand (hereafter denoted by L; see Fig. S1) in water. This ligand was selected because it is well documented experimentally and represents an interesting system to test current simulation techniques as potential tools to design new ligands. Structural information on its complexes with alkaline-earth and lanthanide cations is available, both in the solid state (for Ca^{2+},[8] Ba^{2+},[9] La^{3+}, Eu^{3+} [10] and Yb^{3+} [11]) and in aqueous solution (for M^{2+}, La^{3+}, Eu^{3+} and Lu^{3+} [12–20]). In these 1 : 1 complexes, the cation binding mode involves the two nitrogen atoms and four monodentate carboxylate groups of L. Each complexed cation is also hydrated by one to three water molecules. The stability constants of EDTA complexes with M^{2+} or M^{3+} cations have been determined accurately.[2,21] As shown in Table 1, their entropic component $T\Delta S$ is positive (from 6 to 8 kcal mol^{-1} in the M^{2+} series and from 18 to 24 kcal mol^{-1} in the M^{3+} series), and of larger magnitude than the enthalpic component (from −4 to −7 kcal mol^{-1} in the M^{2+} series and −1 to −3 kcal mol^{-1} in the M^{3+} series).

Table 1 Experimental binding data[a] for $EDTA^{4-}$ in water

	log *K*	ΔH/kcal mol^{-1}	$T\Delta S$/kcal mol^{-1}
Ca^{2+}	10.6[c]	−6.6[b]	7.7[c]
Sr^{2+}	8.7[c]	−4.1[b]	7.7[c]
Ba^{2+}	7.8[c]	−4.9[b]	5.7[c]
La^{3+}	15.5[c]	−2.9[c]	18.2[c]
Eu^{3+}	17.3[c]	−2.6[c]	21.1[c]
Lu^{3+}	19.8[c]	−2.5[c]	24.4[c]

[a] Data reviewed by Martell *et al.* [Ref. 2] for an ionic force of 0.1 mol L^{-1} at [b] 20 °C or at [c] 25 °C.

Our main goals are first to investigate the conformation of $EDTA^{4-}$ uncomplexed in water in the presence of neutralizing counterions (of M^+, M^{2+} or M^{3+} type), in order to determine its conformation and to test whether spontaneous complexation will take place during the simulation. Then, two series of inclusive cation complexes are simulated in water. The first series deals with alkaline-earth M^{2+} cations (Ca^{2+}, Sr^{2+}, Ba^{2+}) while the second one deals with typical "large", "average" and "small" lanthanide cations, *i.e.* La^{3+}, Eu^{3+} and Lu^{3+}. In each series, the cation binding mode and solvation are investigated and compared to available structures in the solid state or in solution. Furthermore, based on free energy perturbation (FEP) simulations, relative binding affinities are determined.

When our work started, no molecular mechanics force field was available for the series of M^{3+} cations that could be used with FEP calculations implemented in AMBER. Most of the MD studies considered a single cation. For instance, Wipff *et al.*[22,23] and van Veggel *et al.*[24] simulated Eu^{3+} complexes with neutral ligands, where Eu^{3+} was modeled with the van der Waals parameters of a Na^+ cation. Fossheim *et al.*[25–27] studied Gd^{3+} complexes of DOTA and derivatives in water, using cation parameters fitted on corresponding crystal structures. These

† **Fig. S1** Schematic representation of $EDTA^{4-}$ (L); **Fig. S2** Calculated lanthanide–water $M^{3+}\cdots O_w$ distances, in Å, and lanthanide coordination numbers CN as a function of r^* (Å) and ε (kcal mol^{-1}) cation parameters; **Fig. S3** The uncomplexed L and L,Na^+ systems: angle NC–CN as a function of time; **Fig. S4** FEP calculations of *endo* $L{\cdot}M^{3+}$ complexes in water: ΔG_4 as a function of λ. La^{3+}–Eu^{3+}; La^{3+}–Lu^{3+}; Eu^{3+}–Lu^{3+} mutations; available as supplementary data. For direct electronic access see http://www.rsc.org/suppdata/p2/a908879b otherwise available from BLDSC (SUPPL. NO. 57690, pp. 6) or the RSC Library. See Instructions for Authors available *via* the RSC web page (http://www.rsc.org/authors).

DOI: 10.1039/a908879b

Table 2 Simulation conditions of M^{n+} cations in water: box size, number of water molecules, simulated times, cutoff conditions. The last column concerns number of windows used in the free energy calculations, the unspecified parameters being the same as in the MD simulations

	MD					Mutations
Cations	Box size/Å^3	No. water	Time/ps	Cutoff/Å	Ewald	Windows
M^{3+} fitting	24.4^3	395	50	10	No	11
La^{3+}, Eu^{3+}, Lu^{3+}	34.4^3	1158	200	15	Yes	41
Ba^{2+}, Sr^{2+}, Ca^{2+}	34.4^3	1158	200	15	No	41
Ba^{2+}, Sr^{2+}, Ca^{2+}	34.4^3	1158	200	15	Yes	41

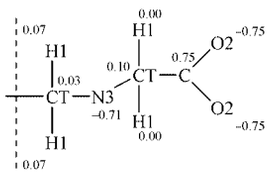

Fig. 1 AMBER atom types and charges on $EDTA^{4-}$ (L).

Gd^{3+} parameters were used by Horrocks *et al.* to simulate Eu^{3+} complexation by potential MRI contrast agents[28] while Judson *et al.* fitted Gd^{3+} parameters to simulate the Gd^{3+} complex of L.[29] Merbach *et al.*[30–32] derived lanthanide parameters from hydration enthalpies and described the static and dynamic features of cation hydration, showing the importance of mimicking the solvent polarization in the first coordination shell. Unfortunately, their parameters, like those used by Meier *et al.*,[33] are not consistent with the standard AMBER force field. Recently, QM simulations "in the gas phase" on the Gd^{3+} complex of DOTA[34] and the Yb^{3+} complex of a DOTA derivative[35] have been reported. None of these studies tackled the question of cation binding selectivity. We therefore developed lanthanide parameters to be used in AMBER, at relatively low computer cost. When our work was completed, another set of parameters for La^{3+}, Eu^{3+} and Yb^{3+} was published by van Veggel *et al.*[36]

The paper is organized as follows. The question of parameter fitting is discussed in the method section. In the results part, we describe L uncomplexed and the M^{2+} and M^{3+} complexes of L. The alkaline-earth cations have been considered because they are often mimicked by luminescent M^{3+} lanthanide cations in biological systems or in their models[37] and because of the availability of force field parameters.[38] Although their complexes are expected to display less charge transfer and polarization effects than the lanthanide complexes, prediction of their binding properties with L remains a challenging task due to the high negative charge of the ligand and to the entropic origin of the stability constants. We thus compare the structures of lanthanide and alkaline-earth complexes with L in aqueous solution, calculated consistently by MD. In the two cation series, the question of cation discrimination by L is tackled by free energy calculations in water.

Methods

Energy representation

All calculations were carried out with the AMBER5.0 software,[39] using the following representation of the potential energy U:

$$U = \Sigma_{\text{bonds}} K_r (r - r_{\text{eq}})^2 + \Sigma_{\text{angles}} K_\theta (\theta - \theta_{\text{eq}})^2 + \Sigma_{\text{dihedrals}} \Sigma_n V_n (1 + \cos n\varphi) + \Sigma_{i<j} (q_i q_j / r_{ij} - 2\varepsilon_{ij} (r_{ij}^*/r_{ij})^6 + \varepsilon_{ij} (r_{ij}^*/r_{ij})^{12})$$

The deformation energies of the bonds (r) and bond angles (θ) are described by harmonic terms. Torsional terms are associated to the dihedral and improper angles (φ). The non-bonded interactions are represented by Coulomb and Lennard-Jones 1–6–12 pairwise additive potentials where r_i^* and ε_i are the van der Waals parameters of atom i. All interactions involving the cations were represented by 1–6–12 potentials, using integer +1, +2 and +3 charges on alkali, alkaline-earth, and lanthanide cations, respectively. In contrast to covalent representations of the metal–ligand interactions,[40–42] our non-covalent model allows for ligand exchange around the cation during the simulation. We used the alkali and alkaline-earth cation parameters of Åqvist,[38] consistent with the AMBER force field. The lanthanide parameters were determined in this study (*vide infra*). The water molecules were represented explicitly with the TIP3P model[43] fitted on the pure liquid phase properties. The atom types for L are described in Fig. 1. The corresponding force field parameters were taken from a Cornell *et al.* force field.[44]

Atomic charges on L are shown in Fig. 1. They were adapted from those calculated on $(CH_3)_2NCH_2CH_2N(CH_3)_2$ and $[HN(CH_2COO)_2]^{2-}$ (RESP fitting[45] of electrostatic potentials from HF/6-31G* calculations).[46]

The solutes were immersed at the center of a cubic solvent box represented with periodic boundary conditions. In most cases, the non-bonded interactions were calculated with a 15 Å cutoff, using the Particle Mesh Ewald (PME) method[50] to account for the long range electrostatic energy components. For time saving purposes, however, other calculations (referred to later as "standard", in short "std") were performed without Ewald, sometimes using a smaller cutoff. Details are given in Tables 2 and 3.

Molecular dynamics (MD) simulations

After 1000 steps of minimization of the systems, the temperature was raised from 100 to 300 K in about 30 ps and MD simulations were carried out at constant pressure and temperature (P = 1 atm, T = 300 K), with a 2 fs time step, constraining C–H and O–H bonds with the SHAKE procedure.[51]

Structural and energetic characteristics of systems were analyzed from trajectory sets saved every 0.5 ps, with MDS,[52] DRAW[53] and INSIGHT-II[54] softwares. The hydration structures of the cations were characterized by the Radial Distribution Functions (RDF) of water (oxygen and hydrogen atoms). Details on calculation conditions (sizes of water box and cut-off, simulated times) are summarized in Tables 2 and 3.

Free energy calculations

The difference in Gibbs free energies (ΔG) between systems A (cation-1) and B (cation-2) were calculated with the Free Energy Perturbation (FEP) method in the standard simulations (no Ewald) while the Thermodynamics Integration (TI) method was used for calculations using PME. Indeed, PME is not implemented in AMBER5.0[39] for FEP calculations. Both FEP and TI methods were combined with a windowing technique, based on the following equations:

TI method:

$$\Delta G = \int_{\lambda=0}^{1} \left\langle \frac{\partial U}{\partial \lambda} \right\rangle_\lambda d\lambda$$

Table 3 Simulation conditions of L and L,M^{n+} systems in water: box size, number of water molecules, simulated times, cutoff conditions. The last two columns concern the number of windows and the cutoff conditions used for the free energy calculations, the unspecified parameters being the same as in the MD simulations

	MD				ΔG_4	
Systems	Box size/Å^3	No. water	Time/ns	Cutoff[a]/Å	Windows	Cutoff[a]/Å
L initially uncomplexed						
L	37^3	1666	1.0	12std		
L,4Na^+	40^3	1977	1.0			
L,Ca^{2+},2Na^+	40^3	1977	0.9[b]	12std	21	12std[f]
			2.0[c]			
L,Eu^{3+},Na^+	40^3	1977	0.9	12 + Ewald		
endo Complexes						
L·M^{2+},2Na^+	46^3	2910	0.2	15std	21	12std
				15 + Ewald[e]	21[g]	15std[g]
					41[g]	15 + Ewald[g]
L·M^{3+},Na^+	45^3	2822	0.4[d]	15 + Ewald	81	15std
			1.0[d]		81	15 + Ewald[h]

[a] Cutoff distances for van der Waals and electrostatic interactions: standard calculations (std: no Ewald) or Ewald calculations (+Ewald). [b] In this simulation, no complexation occurs. [c] In this simulation, an *exo* complex forms after 0.3 ns. [d] 0.4 ns for L·Eu^{3+} and L·Lu^{3+}; 1.0 ns for L·La^{3+}. [e] Only the L·Ca^{2+} complex has been simulated with Ewald. [f] Mutations performed: L·Ca^{2+} to L·Sr^{2+} and L·Ca^{2+} to L·Ba^{2+} (*exo* complexes). [g] Mutation of L·Ca^{2+} to L·Sr^{2+} performed with standard conditions and 21 windows, as well as with Ewald and 41 windows. [h] Only the mutation of L·La^{3+} to L·Lu^{3+} has been performed with Ewald.

FEP method:

$$\Delta G = \Delta G_\lambda \quad \text{and} \quad \Delta G_\lambda = RT \,\mathrm{Log} \left\langle \exp \frac{(U_\lambda - U_{\lambda+\Delta\lambda})}{RT} \right\rangle_\lambda$$

At each window (*i.e.* at each λ), 1 ps of equilibration and 4 ps of data collection were performed and 11 or 81 equally spaced windows were used.

The variations of the potential energy U_λ were calculated using a linear combination of the ε_{ij} and r_{ij}* parameters of the initial state ($\lambda = 1$) and the final state ($\lambda = 0$):

$$\varepsilon(\lambda) = \lambda\varepsilon(1) + (1 - \lambda)\,\varepsilon(0)$$

$$r^*(\lambda) = \lambda r^*(1) + (1 - \lambda)\, r^*(0)$$

For FEP simulations, ΔG's were accumulated "forward" and "backward". Moreover, in most cases, both $\Delta G_{\mathbf{A}\rightarrow\mathbf{B}}$ and $\Delta G_{\mathbf{B}\rightarrow\mathbf{A}}$ energies were calculated separately, starting respectively from state A and from state B, after MD equilibration. We report the average values.

Derivation of the van der Waals lanthanide cation parameters

In the 1–6–12 model we used to describe the M^{3+} lanthanide cations, the "size" of the cation, the resulting cation–ligand distances and interaction energies are determined by the r* and ε cation parameters. They were derived in a stepwise procedure, based on the experimental $M^{3+}\cdots O_w$ distances in solution (X-ray, EXAFS and neutron diffraction studies[18,55–64]), as well as on differences in cation hydration energies reported by Rizkalla *et al.*[65] According to Table 4, the $M^{3+}\cdots O_w$ distances are within 0.02 Å the same with both methods and range from about 2.58 Å for La^{3+} to 2.34 Å for Lu^{3+}. The coordination number (CN) changes from about 9 (La^{3+}) to 8 (Lu^{3+}) in diluted solutions, but displays more versatility, depending on the method used.

Following the procedure adopted by Merbach *et al.*,[30] the r* and ε cation parameters were first systematically varied to investigate how they determine the CN's and the $M^{3+}\cdots O_w$ distances in pure water solution. This was achieved by a series of about 300 MD simulations of 50 ps each (Table 2), where r* was varied from 1.40 to 2.10 Å and ε from 0.005 to 0.110 kcal mol^{-1}. Details are available from the authors on request. The results are depicted in Fig. S2 where the $M\cdots O_w$ distances and CN's are plotted as a function of (r*; ε). It can be seen that there is no unique choice of parameters that reproduces experimental changes in CN's and in $M\cdots O_w$ distances.[18,55–64] Additional criteria were thus needed.

We therefore performed FEP calculations on the difference in hydration free energies ($\Delta\Delta G^{hyd}$) between two cations, using selected (r*; ε) couples and a standard cutoff of 10 Å (no Ewald). Several sets of parameters were found to suitably

Table 4 Hydration characteristics of large, average and small lanthanide cations: cation–oxygen distances (Å) and coordination number (CN) obtained from X-ray and EXAFS studies on aqueous solutions

	X-Ray		EXAFS	
	$M\cdots O_w$	CN	$M\cdots O_w$	CN
La^{3+}	2.58[a]	9.1[a]	2.55[d]	
Eu^{3+}	2.45[a]	8.3[a]	2.43[b,d]–2.44[c]	8.6[b,c]
Gd^{3+}			2.41[b,d]–2.42[c]	7.6[b]–8.0[c]
Lu^{3+}	2.34[a]	8.0[a]	2.31[b]–2.32[c,d]	7.7[b]–7.5[c]

Data from [a] Habenschuss *et al.* [refs. 55–57], [b] Yamaguchi *et al.* [ref. 62], [c] Yaita *et al.* [ref. 61], and [d] David *et al.* [ref. 63].

Table 5 Lanthanide M^{3+} ions in water: final Lennard-Jones r* (Å) and ε (kcal mol^{-1}) parameters, experimental (exp) and calculated (calc) hydration free energies (relative to La^{3+}; kcal mol^{-1}), cation–water $M\cdots O_w$ distances (Å) and cation hydration numbers (CN). Calculated average values and their fluctuations (±) are obtained from the last 100 ps of MD

		La^{3+}	Eu^{3+}	Lu^{3+}
r*		1.90	1.65	1.40
ε		0.065	0.075	0.085
$\Delta\Delta G^{hyd}$	calc	0	−49.8 ± 0.3	−98.6 ± 0.3
	exp	0	−49[a]	−99[a]
$M\cdots O_w$	calc	2.53 ± 0.02	2.36 ± 0.02	2.21 ± 0.02
	exp	2.58[b]	2.45[b]–2.43[c]	2.34[b]–2.31[c]
CN	calc	9.3 ± 0.1	8.9 ± 0.1	8.0 ± 0.1
	exp	9.1[b]	8.3[b]–8.6[c]	8.0[b]–7.5[d]

Data from [a] Rizkalla *et al.* [ref. 65], [b] Habenschuss *et al.* [refs. 55–57], [c] Yamaguchi *et al.* [ref. 62] and [d] Yaita *et al.* [ref. 61].

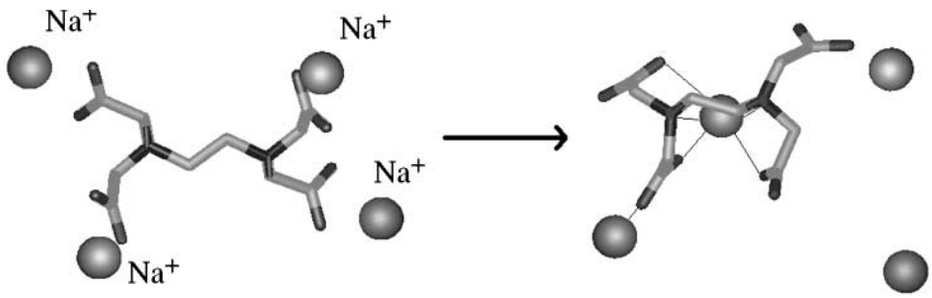

Fig. 2 The uncomplexed (L,4Na$^+$) system at 0 ps (*left*) and 0.9 ns (*right*).

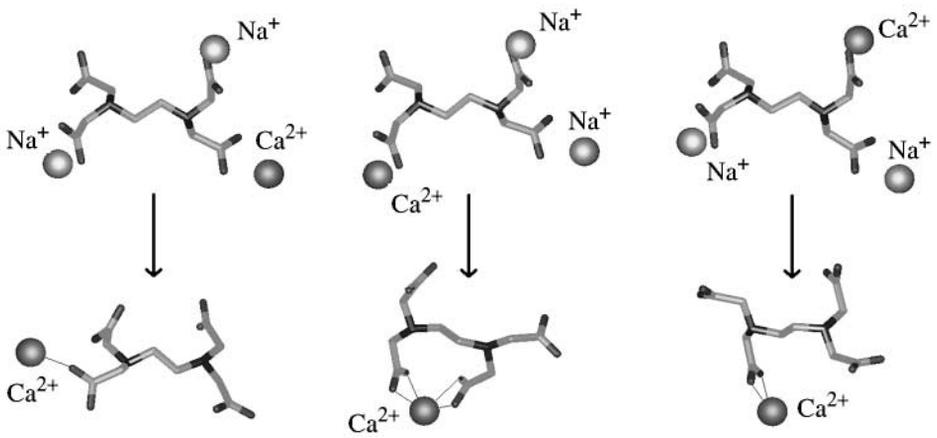

Fig. 3 The uncomplexed (L,Ca^{2+},2Na$^+$) system: starting (*top*) and final (*bottom*) structures. The dissociated Na$^+$ cations are not shown.

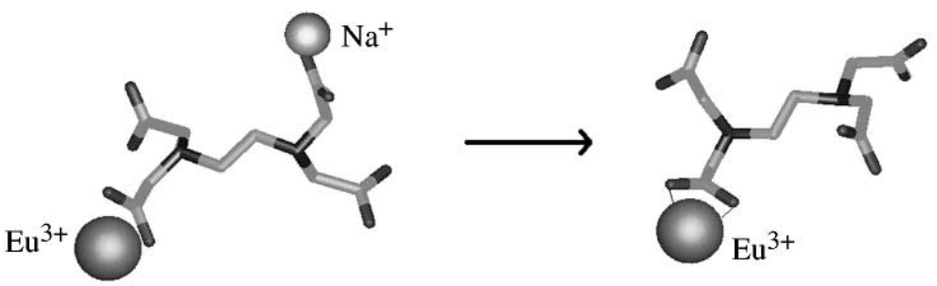

Fig. 4 The uncomplexed (L,Eu^{3+},Na$^+$) system at 0 ps (*left*) and 0.9 ns (*right*; dissociated Na$^+$ is not shown).

model La^{3+}, Eu^{3+} and Lu^{3+}. The final selection was made using the following considerations: (i) as the ionic radius of La^{3+} (1.22 Å [66]) is smaller than that of Ba^{2+} (1.50 Å [66]) r^*_{La} should be smaller than r^*_{Ba} (2.12 Å [38]); (ii) r^* should decrease from La^{3+} to Lu^{3+}, following the ionic radii; (iii) ε increases while r^* decreases, following the same trend as the Åqvist's parameters [38] for the alkali and alkaline-earth cations. Longer simulations (200 ps) using Ewald performed with the parameters selected for La^{3+}, Eu^{3+}, Lu^{3+} confirmed their validity. Minor differences were found with the results obtained with the 10 Å cutoff without Ewald correction. The final cation parameters, the corresponding calculated hydration energies, the characteristics of ion–oxygen RDF's, and experimental data are given in Table 5. Our parameters lead to a good agreement with most experimental structural and energetic data. The only exception concerns the Lu^{3+}–O_w calculated distance (2.21 ± 0.02 Å), which is slightly shorter than the experimental one (2.31 to 2.34 Å).[67]

Results and discussion

Salts of EDTA^{4-} uncomplexed in water

L uncomplexed was simulated in water starting from its *trans* conformer (see initial structures in Figs. 2, 3 and 4), first alone, then in the presence of several types of neutralizing counterions (Na$^+$, Ca^{2+}, Eu^{3+}). We wanted to investigate whether spontaneous cation complexation takes place, in particular with M^{2+} and M^{3+} cations which form stable complexes with L. Complexation implies a *trans* to *gauche* interconversion of L, a high energy process in the gas phase, due to the electrostatic repulsions between the carboxylate groups. The counterions were initially positioned at about 2.4 Å from the two oxygens of a carboxylate group. These simulations were performed with a 12 Å cut-off, for timescales ranging from 0.9 to 2.0 ns. A standard treatment of electrostatics (no Ewald) was used for all systems, except for L,Eu^{3+},Na$^+$, where electrostatic interactions are highest. For the L,4Na$^+$ system, Ewald *vs.* No-Ewald calculations were also compared. Details are given in Table 2.

In the absence of counterions, the L ligand simulated for 1 ns displayed a marked flexibility in water, with conformational changes of the 11 dihedral angles. Focusing on the central NC–CN dihedral, which contributes to the preorganization of the ligand for complexation, it can be seen (Fig. S3) that L is most often *trans* (180°), but undergoes some short excursions to *gauche* forms (60°). In these latter, a water molecule bridging over the N···N atoms of L is found to bring some stabilization.

During the simulation of the L,4Na$^+$ system, one Na$^+$ cation was spontaneously captured by the ligand, which moved from a *trans* to a *gauche* conformation at about 0.6 ns (Figs. S3 and 2). The complex was of inclusive type, involving the two nitrogen atoms and three carboxylate arms only, instead of four as in the Eu^{3+} or Ca^{2+} solid state analogs. The three other Na$^+$ cations

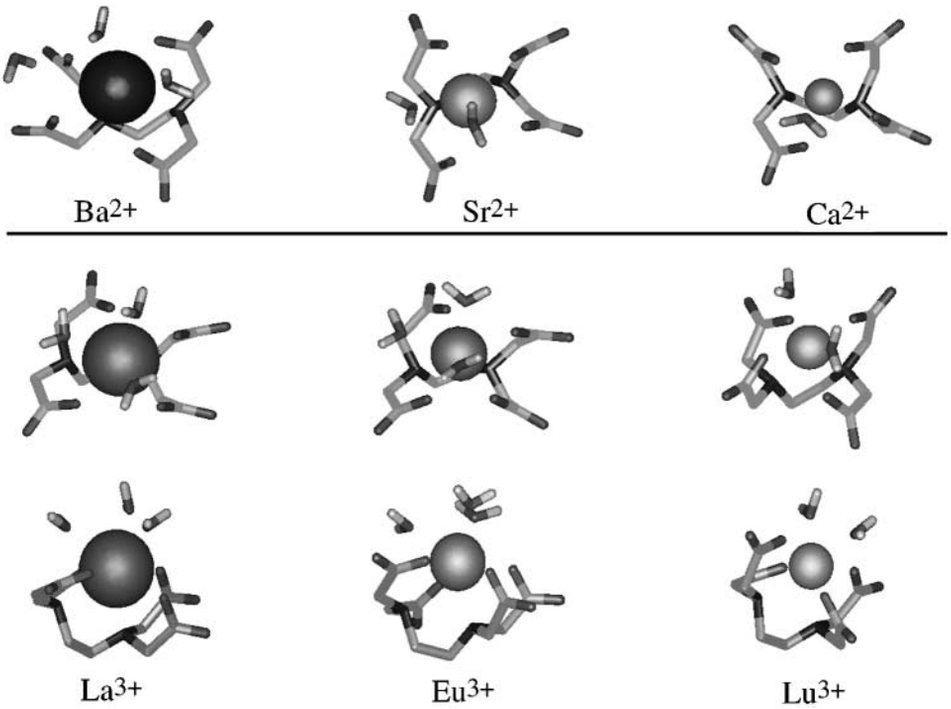

Fig. 5 $L{\cdot}M^{2+}$ and $L{\cdot}M^{3+}$ *endo* complexes: typical structures in water, with selected water molecules (orthogonal views for $L{\cdot}M^{3+}$ complexes).

diluted in water. Interestingly, prior to the Na^+ capture by L (*i.e.* in the first 0.6 ns; Fig. S3), the ligand oscillated between *trans* and *gauche* forms, as noted above for the isolated ligand, indicating that there is not strong effective repulsion betwen the negatively charged arms in water. When this simulation was repeated with Ewald for 2 ns, similar events were observed: three Na^+ cations slowly migrated to the bulk water, while the fourth Na^+ was also captured by the ligand, somewhat later (at about 1.6 ns) than in the standard calculation.

The systems containing Ca^{2+} or Eu^{3+} as counterions behave differently, as no cation complexation took place (Figs. 3 and 4). These cations remained close to carboxylate groups while the additional Na^+ cations moved to the bulk, and the NC–CN dihedral of L remained *trans* throughout the simulations.

For the $L,Ca^{2+},2Na^+$ system, three different starting configurations were tested, where the ligand was *trans* and the Na^+ and Ca^{2+} ions were placed at different locations, close to the carboxylates (Fig. 3). After 0.9 ns, these configurations led to different structures, indicating that the sampling was still not long enough. In all cases, the Ca^{2+} cation formed an intimate ion pair with one to two carboxylates, but never formed inclusive complexes. The ligand remained *trans*. In one case, interestingly, one Ca^{2+} bound bidentately to two arms of the ligand (at about 0.3 ns), forming an *exo* complex which remained bound until the end of the simulation (1.7 ns; see Fig. 3).

Thus, despite the high stability of the M^{2+} and M^{3+} complexes, the latter did not form spontaneously during the simulation in water. This can be explained by the high energy cost related to the cation dehydration process, rather than by the conformational reorganization of L from *trans* to *gauche* as these two forms exchange in water (see L and $L,4Na^+$ systems). This is why we built models of *endo* complexes of these cations with L and simulated them in water (see next section).

Endo complexes of alkaline-earth and lanthanide ions with $EDTA^{4-}$ in water: structures and solvation

In this section, we report the solution behavior of M^{2+} and M^{3+} *endo* complexes of $EDTA^{4-}$, with a particular focus on cation coordination and structural changes as a function of the cation charge and size. The Ca^{2+}, Ba^{2+}, Sr^{2+} and La^{3+}, Eu^{3+}, Lu^{3+} 1 : 1 complexes were simulated for timescales ranging from 0.2 to 1 ns (Table 3). They will be denoted by the following: $L{\cdot}M^{2+},2Na^+$ or $L{\cdot}M^{3+},Na^+$. The initial structures were that of the europium complex in the solid state,[10] where the cation coordinates in a monodentate mode the four carboxylate groups and the two N atoms of L, the NC–CN dihedral being *gauche* (63°). No water molecule was initially coordinated to the cation. Neutralizing Na^+ counterions were placed in the vicinity of carboxy groups of L. During all dynamics, as in the systems described above, the Na^+ ions moved away from the ligand, and will not therefore be discussed further. The $L{\cdot}M^{2+},2Na^+$ complexes were simulated with a standard procedure for the treatment of electrostatics (15 Å cutoff; no Ewald), while $L{\cdot}M^{3+},Na^+$ complexes were simulated with Ewald and a 15 Å cutoff. An additional test with Ewald was also performed on the $L{\cdot}Ca^{2+},2Na^+$ complex.

Cation–ligand distances. *Endo* complexation of the cation rigidifies the ligand, which retained its starting conformation throughout the dynamics (0.2 to 1 ns), while the complexed cations remained coordinated to four monodentate carboxylate groups and to two nitrogen atoms of L. This binding mode is consistent with the one characterized in aqueous solution, as determined by IR, Raman and proton NMR studies of M^{2+} and M^{3+} [12–14] complexes. The calculated fluctuations on the $M\cdots O$ and $M\cdots N$ distances are small (less than 0.1 Å). In all complexes the average $M\cdots N$ distances are somewhat larger than the $M\cdots O$ distances (by about 0.2 Å), but still indicate a significant contribution of the nitrogen binding sites. As expected, these distances decrease with the ion size. $M^{2+}\cdots O$ and $M^{2+}\cdots N$ distances range from 2.27 to 2.74 Å, and from 2.45 to 2.83 Å, respectively, while $M^{3+}\cdots O$ and $M^{3+}\cdots N$ distances range from 2.07 to 2.44 Å and from 2.57 to 2.70 Å, respectively. Comparison of these values with those available from solid state structures of the simulated and of the Nd^{3+} [68] complexes (see Tables 6 and 7) shows that the former are somewhat shorter. The difference ranges from 0.01 Å for the Ba^{2+} complex to 0.19 Å for the Lu^{3+} complex.

Whether the solid state structures are representative of structures in solution remains a matter of debate. Recently, EXAFS studies have been independently reported by Yamaguchi *et al.*[18] and den Auwer *et al.*[19] on the La^{3+}, Gd^{3+} (which has nearly the

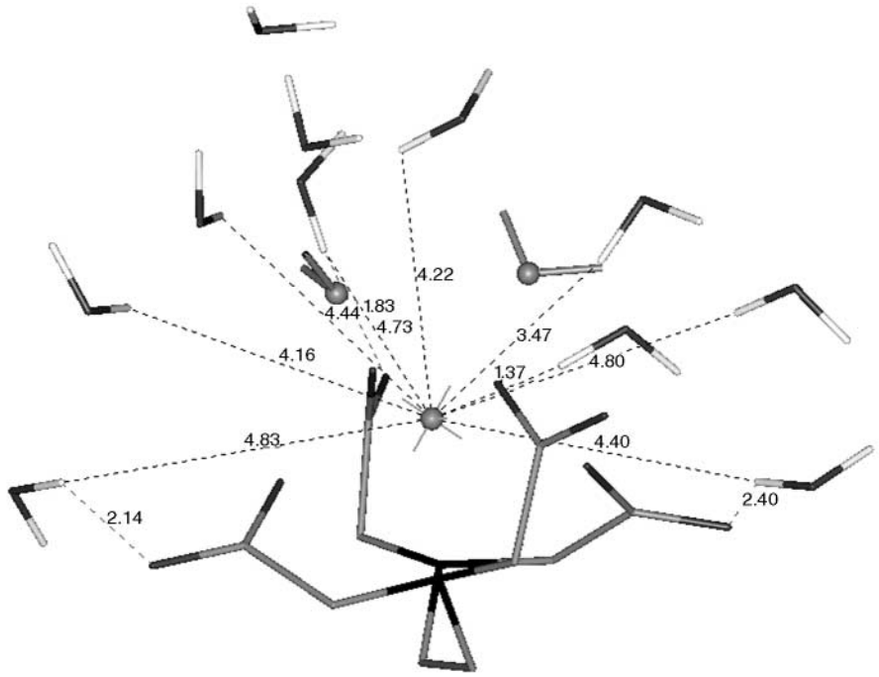

Fig. 6 $L{\cdot}Lu^{3+}$ *endo* complexes: selected first shell water molecules.

Table 6 Geometrical features of $L{\cdot}M^{2+}$ and $L{\cdot}M^{3+}$ *endo* complexes: structures calculated in water (calc) and solid state structures (exp). Average distances (Å), dihedrals (°) and cation hydration numbers CN_{ow} are obtained by MD after equilibration

		$Ba^{2+\,a}$	Sr^{2+}	$Ca^{2+\,b}$	$La^{3+\,c}$	$Eu^{3+\,c}$	$Lu^{3+\,d}$
M···O	calc	2.74 ± 0.10	2.52 ± 0.10	2.27 ± 0.07	2.44 ± 0.06	2.28 ± 0.05	2.07 ± 0.04
	exp	2.75	—	2.37 ± 2.45	2.49 ± 0.04	2.41 ± 0.02	2.26 ± 0.01
M···N	calc	2.83 ± 0.09	2.63 ± 0.09	2.45 ± 0.08	2.70 ± 0.10	2.63 ± 0.11	2.57 ± 0.14
	exp	2.99	—	2.62–2.71	2.77 ± 0.04	2.67 ± 0.03	2.53 ± 0.01
$M\cdots O_w$	calc	2.77 ± 0.02	2.58 ± 0.02	2.37 ± 0.02	2.54 ± 0.02	2.40 ± 0.02	2.26 ± 0.02
	exp	—	—	2.45	2.59	2.49	2.37
NC–CN	calc	60 ± 7	56 ± 8	50 ± 7	57 ± 6	55 ± 6	53 ± 6
	exp	41	—	58	65	63	55
CN_{Ow}	calc	3.0 ± 0.1	2.0 ± 0.1	1.0 ± 0.1	3.0 ± 0.1	2.9 ± 0.1	2.0 ± 0.1
	exp	—	—	—	3	3	2

Crystal structures: [a] $(L,2Ba^{2+},2.5H_2O)$ from Meicheng *et al.* [ref. 9]; [b] $(L,2Ca^{2+},7H_2O)$ from Barnett *et al.* [ref. 8]; [c] $(L,La^{3+},K^{+},3H_2O)$ and L,Eu^{3+}, $Na^{+},3H_2O)$ from Nakamura *et al.* [ref. 10]; [d] $(L,Yb^{3+},Cs^{+},3H_2O)$ from Nassimbeni *et al.* [ref. 11].

Table 7 Average cation–EDTA distances (Å) from XAFS experiments in aqueous solution, from crystal structures, and from our simulations

	EXAFS (aqueous solution)	X-Ray (crystal)	Our simulations (aqueous solution)
La^{3+}	2.48 [a]	2.59 [e]	2.53
Nd^{3+}	2.54 [b,c]–2.41 [a,c]	2.53 [f]	—
Eu^{3+}	2.44 [b,d]–2.37 [a,d]	2.49 [e]	2.40
Dy^{3+}	2.39 [b]–2.29 [a]	2.47 [g]	—
Lu^{3+}	2.33 [b]–2.25 [a]	2.36 [g]	2.27

XAFS results from [a] Yamaguchi *et al.* [ref. 18] and from [b] den Auwer *et al.* [ref. 19]. [c] Electronic parameters and fitting process were tested on the crystal of $L{\cdot}Nd^{3+}$. [d] For the $L{\cdot}Gd^{3+}$ complex. Crystal structures from [e] Nakamura *et al.* [ref. 10], [f] Matkovic-Calogovic [ref. 68], [g] Nassimbeni *et al.* [ref. 11] (for $L{\cdot}Yb^{3+}$ complex).

size of Eu^{3+}) and Lu^{3+} complexes with L in aqueous solution. These studies cannot distinguish between nitrogen and oxygen coordination to the cation. Interestingly, there is no quantitative agreement between their cation–ligand distances, those of den Auwer *et al.* being about 0.08 Å larger than those of Yamaguchi *et al.* (Table 7). For a given cation, both sets of average distances are also very close to those in the solid state structure, but are about 0.1 Å shorter. We notice that differences between experimental distances are larger than the difference between our calculated values and, for instance, those in the solid state. Thus, further discussions about the quantitative assessment of the calculated structures are of little relevance. When comparison can be made, we notice that our distances lie in between those determined by the two EXAFS studies.

Hydration of the complexed cation. Another matter of interest concerns the hydration of the complexed cation. According to the analysis of RDF's obtained from the simulated trajectories, the cation coordinates to water molecules, whose number N_{wat} increases with the cation size. N_{wat} equals 1 for Ca^{2+}, 2 for Sr^{2+} and Lu^{3+}, and 3 for Ba^{2+}, Eu^{3+} and La^{3+} (Figs. 5 and 6). Visual inspection of the trajectories reveals that this coordination lasts during the whole simulation. These results are fully consistent with hydration patterns in the crystalline state [10,11] where N_{wat} equals 3 for La^{3+} and Eu^{3+} and 2 for Yb^{3+}. In solution, luminescence studies [16,17] confirm that N_{wat} is 3 for Eu^{3+}, as in our simulation. A similar hydration ($N_{wat} = 3$) has been found in the MD simulations of Judson *et al.*[29] on the closely related $L{\cdot}Gd^{3+}$ complex.

Concerning the calculated hydration of complexed alkaline-earth cations ($N_{wat} = 1$ for Ca^{2+}, 2 for Sr^{2+} and 3 for Ba^{2+}) comparisons with experiments are more difficult. To our knowledge, no data are available in solution. The solid state structures of the $L{\cdot}Ca^{2+}$ [8] and $L{\cdot}Ba^{2+}$ [9] can hardly be compared with those we

Table 8 $L{\cdot}M^{2+}$ and $L{\cdot}M^{3+}$ *endo* complexes in water: average energy components and their fluctuations (kcal mol^{-1}) obtained after MD equilibration

	Ba^{2+}	Sr^{2+}	Ca^{2+}	La^{3+}	Eu^{3+}	Lu^{3+}
E_L [a]	704 ± 8	723 ± 11	752 ± 8	753 ± 8	783 ± 9	799 ± 9
$E_{M/L}$ [b]	−830 ± 9	−898 ± 10	−989 ± 7	−1381 ± 9	−1472 ± 10	−1586 ± 11
$E_{M/water}$ [c]	77 ± 20	130 ± 23	191 ± 17	−94 ± 22	−110 ± 25	−69 ± 28
$E_{L/water}$ [d]	−507 ± 41	−580 ± 38	−606 ± 28	−265 ± 28	−53 ± 38	−217 ± 36
E_{ML} [e]	−126 ± 8	−176 ± 9	−237 ± 5	−629 ± 7	−689 ± 7	−788 ± 8
$E_{ML/water}$ [f]	−430 ± 27	−450 ± 23	−415 ± 16	−359 ± 19	−352 ± 18	−286 ± 18

[a] Internal energy of L. [b] Cation–ligand interaction energy. [c] Cation–water interaction energy. [d] Ligand–water interaction energy. [e] Total energy of the $M{\cdot}L^{n+}$ complex. [f] Complex–water interaction energy.

simulated, as no discrete complexes can be distinguished in the crystals, the cation being in contact with two ligands. The Ca^{2+} cation is eight coordinated, involving one water molecule and one carboxylate oxygen of another ligand.

Energy component analysis. We analyzed the energy characteristics of the complexes in water. Averages over the last 100 to 400 ps of MD (*i.e.* after equilibration) are reported in Table 8. Two main classes of complexes can be distinguished, depending on the charge of the complexed cation. For a given complex, the internal energy of L (E_L) and the interaction energies of L with the complexed cation ($E_{M/L}$) are quasi-constant along the dynamics (their relative fluctuations are less than 2%). $E_{M/L}$ is about 1.5 times larger for M^{3+} (−1380 to −1590 kcal mol^{-1}) than for M^{2+} (−830 to −990 kcal mol^{-1}) cations, which corresponds to the ratio of their charges. This indicates that all these species involve similar binding modes of the cation. In a given series, as the cation size decreases, the cation/ligand attraction energy ($E_{M/L}$) increases (by about 210 kcal mol^{-1} in the M^{3+} complexes and 160 kcal mol^{-1} in the M^{2+} complexes), while the ligand gets more strained (by about 50 kcal mol^{-1} in both series). For all complexes, the L/water interaction energies ($E_{L/water}$) are attractive, but less with M^{3+} cations (from −220 to −270 kcal mol^{-1}) than with M^{2+} cations (from −510 to −610 kcal mol^{-1}), as the $L{\cdot}M^{2+}$ species are more negatively charged than the $L{\cdot}M^{3+}$ species (−2 and −1, respectively). Thus, *the structure of water around the complex is mostly determined by the ligand, rather than by the complexed cation whose solvation is antagonist*. Indeed, the M^{n+}/water interactions are attractive in the M^{3+} complexes (from −70 to −110 kcal mol^{-1}), but repulsive in the M^{2+} ones (80 to 190 kcal mol^{-1}). This is because the water structure in the second hydration shell of M^{2+} cations is determined by the hydration of carboxylate groups, rather than by the cation: the water protons point towards the cations (see the example of the Lu^{3+} complex in Fig. 6). As expected, the cation/water repulsion energies ($E_{M/water}$) decrease when the number of water molecules in the first hydration shell increases from one to three (from Ca^{2+} to Ba^{2+}). In the case of the lanthanide complexes, two water molecules coordinate to Lu^{3+} while three water molecules coordinate to La^{3+} and Eu^{3+}, leading to total water/cation interactions which are about 35 kcal mol^{-1} more attractive in the latter complexes. Thus, *although the largest cations display intrinsically weaker attractions with bulk water than the smallest ones, they interact more with water within the complex*, due to higher hydration numbers. Finally, comparing the *endo vs. exo* Ca^{2+} complexes, it can be noticed that the gain in water/complex interactions compensates the lower internal stability of the *exo* complex, so that $E_{ML} + E_{ML/water}$ is not very different for *exo* (−685 ± 30 kcal mol^{-1}) and *endo* (−652 ± 20 kcal mol^{-1}) complexes.[69] This suggests that, due to solvation effects, the two forms may be in equilibrium. Interestingly, ultrasonic absorption experiments of Harada *et al.*[20] suggested that the $L{\cdot}Ca^{2+}$ complex exists in two forms in water, one entity having a cation more hydrated than the other.

M^{n+} complexation by $EDTA^{4-}$ in water: cation binding selectivities

According to the thermodynamic cycle shown in the Scheme 1,

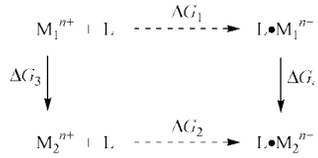

Scheme 1

the binding selectivity of M_1^{n+}, relative to M_2^{n+}, complexed by L in water, obtained experimentally as $\Delta\Delta G_c = \Delta G_1 - \Delta G_2$, can be obtained computationally *via* ΔG_3 and ΔG_4 in solution: $\Delta\Delta G_c = \Delta G_3 - \Delta G_4$. The ΔG_3 and ΔG_4 energies for alkaline-earth and lanthanide cations are reported in Table 9. ΔG_3 corresponds to the difference in free energies of hydration $\Delta\Delta G_{hyd}$ of the uncomplexed cations.

For the uncomplexed M^{2+} cations, the ΔG_3 values obtained from standard calculations (no Ewald) were within 0.2 kcal mol^{-1} identical to those obtained with Ewald, likely because long range forces remain nearly constant throughout the mutations (Table 9). This is why we report one set of ΔG_3's only (Table 9). These values are also within 0.3 kcal mol^{-1} identical to those calculated by Åqvist[38] with a somewhat different solvent representation, or by Muzet *et al.*[70] with a smaller cutoff (10 Å instead of 15 Å). They also agree within 2 kcal mol^{-1} with experimental data.

The initial structures of the complexes used for the FEP calculations were the final structures of *endo* complexes obtained from the MD simulations, where Na^+ counterions ensure electroneutrality. Most ΔG_3 and ΔG_4 energies were averaged from two independent mutation simulations (M_1^{n+} to M_2^{n+}, and M_2^{n+} to M_1^{n+}). Typical changes of ΔG_4 along the mutation are given in Fig. S4. The values obtained with different cutoff and Ewald conditions, as well as sampling times are given in Table 9 with the corresponding $\Delta\Delta G_c$'s. Most calculations of ΔG_4 used a standard procedure (no-Ewald), with a 12 Å cutoff for M^{2+} complexes and a 15 Å cutoff for the M^{3+} complexes.

The effects of long range electrostatics on ΔG_4 were investigated by additional tests using either larger cutoff or Ewald summation in both cation series. The different Ca^{2+} to Sr^{2+} mutations show that the standard procedure (12 Å cutoff) gives a ΔG_4 of 43.0 ± 0.3 kcal mol^{-1}, close to the values obtained with a standard 15 Å cutoff (44.1 kcal mol^{-1}) or with 15 Å cutoff+Ewald (42.3 kcal mol^{-1}). Similarly, the direct La^{3+} to Lu^{3+} mutations using the standard 15 Å or 15 Å+Ewald conditions lead to very close values of ΔG_4 (−115.5 and −116.7 kcal mol^{-1}, respectively). These comparisons show that long range electrostatic interactions are similar in a given cation series and do not critically determine the cation binding selectivities.

For any pair of ions, whatever the simulation conditions, the ΔG_4 energies are found to be markedly larger than the ΔG_3 energies, leading to the conclusion that *the smallest cation of the*

Table 9 Differences in Gibbs free energy (kcal mol^{-1}) for M^{2+} and M^{3+} cations and their complexes. Unless otherwise indicated, the reported ΔG_3 and ΔG_4 values are averaged from $M_1^{n+} \rightarrow M_2^{n+}$ and $M_2^{n+} \rightarrow M_1^{n+}$ independent mutations: ± is the corresponding difference. With one exception,[c] all complexes are *endo*

	ΔG_3[a]	ΔG_4			$\Delta\Delta G_c$	
$M_1^{n+} \rightarrow M_2^{n+}$	Energy	Energy	Cutoff	Windows	Calc	Exp[d]
$Ca^{2+} \rightarrow Sr^{2+}$	35.3 ± 0.3	43.0 ± 0.3	12std	21	−7.7 ± 0.6	−2.6
		44.1[b]	15std	21	−8.8	
		42.3[b]	15+Ewald	41	−7.0	
$Ca^{2+} \rightarrow Ba^{2+}$	67.4 ± 0.3	80.5 ± 1.9	12std	21	−13.1 ± 2.2	−3.8
$Sr^{2+} \rightarrow Ba^{2+}$	31.4 ± 0.3	37.3 ± 0.8	12std	21	−5.9 ± 1.1	−1.2
$Ca^{2+} \rightarrow Sr^{2+}$	35.3 ± 0.3	39.4[b,c]	12std	21	−4.1	−2.6
$Ca^{2+} \rightarrow Ba^{2+}$	67.4 ± 0.3	73.5[b,c]	12std	21	−6.1	−3.8
$La^{3+} \rightarrow Lu^{3+}$	−98.6 ± 0.3	−119.1 ± 6.9	15std	81	20.5 ± 7.2	5.8
		−116.7[b]	15+Ewald	81	18.1	
$La^{3+} \rightarrow Eu^{3+}$	−49.8 ± 0.3	−56.3 ± 0.7	15std	81	6.5 ± 1.0	2.6
$Eu^{3+} \rightarrow Lu^{3+}$	−48.8 ± 0.3	61.8 ± 3.7	15std	81	13.0 ± 4.0	3.2

[a] Obtained with 15 Å cutoff with Ewald. Mutations performed with 41 windows. [b] Single mutation performed from M_1^{n+} to M_2^{n+}. [c] *Exo* complexes. [d] Data from Martell *et al.* [ref. 2].

pair forms a more stable complex with L than the largest one in water. As a result, in each cation series, the order of thermodynamic stabilities is found to follow the ionic radius. It also corresponds to the experimental trend. Thus, computations using cation parameters fitted on hydration properties are successful in reproducing the experimental stability order in both cation series, despite the entropic origin of these complexes:[2]

$$L{\cdot}Ca^{2+} > L{\cdot}Sr^{2+} > L{\cdot}Ba^{2+} \quad \text{and} \quad L{\cdot}Lu^{3+} > L{\cdot}Eu^{3+} > L{\cdot}La^{3+}$$

The stabilities are thus mostly determined by the relative interaction energies of the cations with the ligand in water (ΔG_4), rather than by the dehydration energies of the cations (ΔG_3).

The influence of sampling (number of windows used for the calculation of ΔG_4) was also studied in the two series of cations. In the case of M^{2+} complexes, the structures obtained at the end of the mutations are close to those obtained independently by MD. Similar ΔG_4 ($L{\cdot}Ca^{2+} \rightarrow L{\cdot}Sr^{2+}$) values are obtained (within 0.7 kcal mol^{-1}) for calculations performed with either 21 or 41 windows: in both cases, one water molecule exchanges between the bulk and the first coordination sphere of M^{2+}. In the case of lanthanide complexes, water molecules are more strongly coordinated to the cation, which may require enhanced sampling to obtain ΔG_4. Thus, calculations were performed with 81 windows. The largest hysteresis between forward and backward mutations (Fig. S4) is observed when the lanthanide water coordination number changes, *i.e.* during the $L{\cdot}La^{3+} \rightarrow L{\cdot}Lu^{3+}$ and the $L{\cdot}Eu^{3+} \rightarrow L{\cdot}Lu^{3+}$ mutations (3.7 and 6.9 kcal mol^{-1}, respectively). Nevertheless, hydration patterns at the end of these mutations are similar to those obtained by MD of the final system. The only exception concerns the $L{\cdot}Lu^{3+} \rightarrow L{\cdot}Eu^{3+}$ mutation, where Eu^{3+} binds to two water molecules only, *i.e.* by one less than found by MD in the $L{\cdot}Eu^{3+}$ complex. However, the ΔG_4 values obtained from the $L{\cdot}Lu^{3+} \rightarrow L{\cdot}Eu^{3+}$ simulation and from the $L{\cdot}Eu^{3+} \rightarrow L{\cdot}Lu^{3+}$ simulation are of very close magnitude (+63.6 and −60.0 kcal mol^{-1}, respectively), which shows that this change in hydration does not critically determine the cation binding selectivity.

Although trends in binding selectivities are nicely reproduced, the agreement between the calculated and experimental difference in free energy is not quantitative, as the calculated $\Delta\Delta G_c$ (and hence the $\Delta\Delta G_4$) energies are overestimated. Similar FEP simulations[70] on M^{2+} complexes of a neutral calix[4]arene ligand also overestimated the relative selectivities. As shown above, this discrepancy is unlikely to result from deficiencies in the sampling process or in the treatment of long range electrostatics. We believe that this is caused by the neglect of charge transfer from the ligand to the cation, which would scale down the interaction energies and their differences. We notice that the successful tests reported by van Veggel *et al.* on lanthanide complexes of 18-crown-6[36] used a less polar representation of the ligand ($q_O = -0.43$), which also scales down the interaction energies with the cation. According to quantum mechanical calculations on divalent and trivalent cation complexes with neutral ligands, charge transfer amounts to about 0.2 and 0.4 e, respectively per ligand.[71] The charge transfer to a negatively charged ligand is larger.[72] Another difficulty in the modeling of such complexes stems from the fact that the binding selectivity results from small differences between large numbers. Given these difficulties and the simplicity of the force field model used to represent the potential energy of the system, the overall results are quite satisfactory. Another issue, concerning the binding mode of the cation, is examined in the next section.

Influence of *endo*/*exo* coordination mode on binding selectivity

The role of the starting structures on binding selectivities was investigated in the M^{2+} cation series, as two binding modes were characterized from our simulations for the Ca^{2+} complex. FEP simulations were thus rerun starting from the *exo* form of the Ca^{2+} complex described above: Ca^{2+} was initially bound to two bidentate carboxylate groups of L, the two other carboxylate groups being free and the NC–CN dihedral being *anti* (see Fig. 3).

During the $L{\cdot}Ca^{2+} \rightarrow L{\cdot}Sr^{2+}$ and $L{\cdot}Ca^{2+} \rightarrow L{\cdot}Ba^{2+}$ mutations, the complexes remained *exo* as in the starting complex. The new set of calculated $\Delta\Delta G_c$ (Table 9) again reproduces the experimental order of thermodynamic stabilities: $L{\cdot}Ca^{2+} > L{\cdot}Sr^{2+}$ and $L{\cdot}Ca^{2+} > L{\cdot}Ba^{2+}$. Interestingly, the corresponding *exo* selectivities are closer to experimental values than those obtained with *endo* complexes. This suggests, as pointed out by others,[20] that several structures of $L{\cdot}M^{n+}$ complexes co-exist in solution and contribute to the macroscopic binding selectivity. In principle, if the simulations were long enough, all these states should be sampled. As seen for the Ca^{2+} complex, this is not the case, likely because the high interactions with the cation and the ligand lead to high energy barriers for conformational changes and interconversion of binding modes.

Conclusion

Lanthanide and alkaline-earth complexes of $EDTA^{4-}$ were simulated in water by molecular dynamics. For this purpose, a set of parameters has first been derived for La^{3+}, Eu^{3+} and Lu^{3+} cations from energetic and structural considerations of lanthanide hydration. Cation/ligand interactions were represented with a classical 1–6–12 pair potential, with a fixed +3 charge on the lanthanide cations. This model reproduces the variation from nine to eight of the coordination number for aqua com-

plexes along the lanthanide series as well as relative Gibbs free energies of hydration, at reasonable computational times. It has then been used to study $EDTA^{4-}$ complexes. In the *endo* complex type of alkaline-earth and lanthanide cations, the cation is coordinated by four monodentate carboxylate groups and two nitrogen atoms of $EDTA^{4-}$, in agreement with experimental data. In the case of Ca^{2+} cations, however, a second type of complex (*exo*) has been observed where the cation is only coordinated by two bidentate carboxylate groups. The thermodynamic stability order of lanthanide and alkaline-earth $EDTA^{4-}$ complexes is qualitatively reproduced by free energy calculations ($\Delta\Delta G$) in aqueous solution, despite the entropic origin of the complexes. Similar agreement has been obtained with related ligands such as $DOTA^{4-}$ or $MIDA^{2-}$ in aqueous solution.[47] On the methodological side, we have shown that, despite the high charges involved in the simulated systems, Ewald summation has little influence on the results, likely because these interactions are similar in a given series of complexes. More quantitative prediction of binding selectivities and of ion solvation dynamic features requires more elaborate representations of the ligands and solvents, including polarization and charge transfer effects.

Acknowledgements

S. D. acknowledges the CEA for a PhD grant.

References

1 M. F. Loncin, J. F. Desreux and E. Merciny, *Inorg. Chem.*, 1986, **25**, 2646.
2 A. E. Martell and R. M. Smith, *Critical Stability Constants. Amino-Acids*, Plenum Press, New York, 1974–1982.
3 G. Anderegg, *Critical survey of stability constants of EDTA complexes*, IUPAC Chemical Data Series, No. 14, 1976.
4 S. F. Lincoln, *Adv. Inorg. Bioinorg. Mech.*, 1986, **4**, 217.
5 W. W. Schulz and J. D. Navratil, *Recent developments in separation science*, ed. N. N. Li, CRC Press, Boca Raton, FL, 1982.
6 B. Weaver and F. A. Kappelman, *Inorg. Nucl. Chem.*, 1968, **30**, 263.
7 F. A. Kappelman, USP 3 230 036/18 Jan 1966.
8 B. L. Barnett and V. A. Uchtman, *Inorg. Chem.*, 1979, **18**, 2674.
9 S. Meicheng, T. Zengren, L. Tongchang, S. Shiying and Y. Youqi, *Sci. Sinica*, 1979, **XXII**, 912.
10 K. Nakamura, T. Kurisaki, H. Wakita and T. Yamaguchi, *Acta Crystallogr., Sect. C*, 1995, **51**, 1559.
11 L. R. Nassimbeni, M. R. W. Wright, J. C. van Niekerk and P. A. McCallum, *Acta Crystallogr., Sect. B*, 1979, **35**, 1341.
12 A. A. McConnell, R. H. Nutall and D. M. Stalker, *Talanta*, 1978, **25**, 425.
13 P. A. Baisden, G. R. Choppin and B. B. Garrett, *Inorg. Chem.*, 1977, **16**, 1367.
14 R. J. Kula, D. T. Sawyer, S. I. Chan and C. M. Finley, *J. Am. Chem. Soc.*, 1963, **85**, 2930.
15 T. Kimura, Y. Kato and G. R. Choppin, *Workshop on Actinides Solution Chemistry: Separation Chemistry, September 1st and 2nd*, 1994, Tokai, Japan.
16 C. C. Bryden and C. N. Reilley, *Anal. Chem.*, 1982, **54**, 610.
17 M. Latva and J. Kankare, *J. Coord. Chem.*, 1998, **43**, 121.
18 T. Yamaguchi, K. Nakamura, H. Wakita and M. Nomura, in *Recent progress on actinide separation chemistry. Proceedings of the workshop on actinide solution chemistry: separation chemistry, WASC'94, Meeting date 1994*; Z. Yoshida, T. Kimura and Y. Meguro, World Scientific, Singapore, pp. 165–180, 1997.
19 C. den Auwer and S. Durand, unpublished results.
20 S. Harada, Y. Funaki and T. Yasunaga, *J. Am. Chem. Soc.*, 1980, **102**, 136.
21 G. Scharzenbach, R. Gut and G. Anderegg, *Helv. Chim. Acta*, 1954, **117**, 937.
22 P. Auffinger and G. Wipff, *J. Am. Chem. Soc.*, 1991, **113**, 5976.
23 P. Guilbaud, A. Varnek and G. Wipff, *J. Am. Chem. Soc.*, 1993, **115**, 8298.
24 F. C. J. M. van Veggel, M. P. O. Wolbers and D. N. Reinhoudt, *J. Phys. Chem. A*, 1998, **102**, 3060.
25 R. Fossheim and S. G. Dahl, *Acta Chem. Scand.*, 1990, **44**, 698.
26 R. Fossheim, S. G. Dahl and H. Dugstad, *Eur. J. Med. Chem.*, 1991, **26**, 299.
27 R. Fossheim, H. Dugstad and S. G. Dahl, *J. Med. Chem.*, 1991, **34**, 819.
28 S. T. Frey, C. A. Chang, J. F. Carvalho, A. Varadarajan, L. M. Schultze, K. L. Pounds and W. DeW. Horrocks, *Inorg. Chem.*, 1994, **33**, 2882.
29 Y. Tan, R. S. Judson and C. F. Melius, *J. Mol. Model.*, 1996, **2**, 160.
30 S. Galera, J. M. Lluch, A. Oliva, J. Bertran, F. Foglia, L. Helm and A. E. Merbach, *New J. Chem.*, 1994, **17**, 773.
31 C. Cossy and A. E. Merbach, *Pure Appl. Chem.*, 1988, **60**, 1785.
32 T. Kowall, F. Foglia, L. Helm and A. E. Merbach, *J. Am. Chem. Soc.*, 1995, **117**, 3790.
33 W. Meier, P. Bopp, M. M. Probst, E. Spohr and J. I. Lin, *J. Phys. Chem.*, 1990, **94**, 4672.
34 U. Cosentino, G. Moro, D. Pitea, A. Villa, P. C. Fantucci, A. Maiocchi and F. Uggerin, *J. Phys. Chem. A*, 1998, **102**, 4606.
35 Y. H. Jang, M. Blanco, S. Dasgupta, D. A. Keire, J. E. Shively and W. A. Goddard III, *J. Am. Chem. Soc.*, 1999, **121**, 6142.
36 F. C. J. M. van Veggel and D. Reinhoudt, *Chem. Eur. J.*, 1999, **5**, 90.
37 J. M. Harrowfield, M. I. Ogden, W. R. Richmond and A. H. White, *J. Chem. Soc., Dalton Trans.*, 1991, 2153.
38 J. Åqvist, *J. Phys. Chem.*, 1990, **94**, 8021.
39 D. A. Case, D. A. Pearlman, J. C. Caldwell, T. E. Cheatham III, W. S. Ross, C. L. Simmerling, T. A. Darden, K. M. Merz, R. V. Stanton, A. L. Cheng, J. J. Vincent, M. Crowley, D. M. Ferguson, R. J. Radmer, G. L. Seibel, U. C. Singh, P. K. Weiner and P. A. Kollman, *AMBER5*, University of California, San Francisco, 1997.
40 B. Hay, *Inorg. Chem.*, 1991, **30**, 2876.
41 R. D. Hancock, D. E. Reichert and M. J. Welch, *Inorg. Chem.*, 1996, **35**, 2165.
42 P. Comba, *Coord. Chem. Rev.*, 1999, **185–186**, 81.
43 W. L. Jorgensen, J. Chandrasekhar and J. D. Madura, *J. Chem. Phys.*, 1983, **79**, 926.
44 W. D. Cornell, P. Cieplak, C. I. Bayly, I. R. Gould, K. M. Merz, D. M. Ferguson, D. C. Spellmeyer, T. Fox, J. W. Caldwell and P. A. Kollman, *J. Am. Chem. Soc.*, 1995, **117**, 5179.
45 W. D. Cornell, P. Cieplak, C. I. Bayly and P. A. Kollman, *J. Am. Chem. Soc.*, 1993, **115**, 9620.
46 The final choice of q_N (−0.71 e) and q_O (−0. 79 e) charges of the two types of binding sites deserves some comments, as these charges critically determine the relative contributions of the amino and carboxylate groups to the cation binding. Indeed, we found that RESP fitting procedures performed on the whole L ligand, selecting either a single conformation, or a large set of structures generated by MD in the gas phase, led to unbalanced representation of the binding sites, where q_N was too low compared to q_O.[47] An unfortunate consequence was that in the corresponding optimized complexes all cation–nitrogen distances were too long, compared to the solid state structures. In the study of Teleman *et al.*,[48] which used unbalanced charges ($q_O = -0.82$ and $q_N = -0.12$ e), similar artefactual geometrical distortions were also observed. The charges we use do not lead to such an artefact, as shown by the comparison of calculated *vs.* experimental structures. Using *ab initio* calculations on Eu^{3+} and Gd^{3+} complexes with model fragments, we also checked that the relative contributions of amino *vs.* carboxylate binding groups is properly balanced. Other *ab initio* calculations (HF level, with a 6-31G* basis set) on the interaction of $EDTA^{4-}$ "complexed" with point charges of +1, +2 and +3, respectively (no charge transfer) show that the amino group is strongly polarized:[47] the q_N Mulliken charges are −0.56, −0.70 and −0.84 e respectively, while the corresponding q_O charges are −0.79, −0.82 and −0.85 e. Thus, the q_N and q_O charges used throughout this study somewhat mimic polarization effects induced by hard cations. Similar values have been reported recently in an MD study of M^{2+} complexes of $DOTA^{4-}$.[49]
47 S. Durand, *Simulations par mécanique quantique et dynamique moléculaire de la complexation de cations alcalino-terreux et lanthanide par des ligands polyaminocarboxylate*, Thesis, Université Louis Pasteur, Strasbourg, 1999.
48 O. Teleman and P. Ahlström, *J. Am. Chem. Soc.*, 1986, **108**, 4333.
49 A. Varnek, G. Wipff, A. Bilyk and J. Harrowfield, *J. Chem. Soc., Dalton Trans.*, 1999, **23**, 4155.
50 T. A. Darden, D. M. York and L. G. Pedersen, *J. Chem. Phys.*, 1993, **98**, 10 089.
51 J. P. Ryckaert, G. Ciccotti and H. J. C. Berendsen, *J. Comput. Phys.*, 1977, **23**, 327.
52 E. Engler and G. Wipff, unpublished results.
53 E. Engler and G. Wipff, in *Crystallography of Supramolecular Compounds*, ed. G. Tsoucaris, Kluwer, Dordrecht, pp. 471–476, 1996.
54 *INSIGHT-II*, Molecular Simulations Inc., 9685 Scranton Road, CA 92121-3752 San Diego, USA.
55 A. Habenschuss and F. H. Spedding, *J. Chem. Phys.*, 1979, **70**, 3758.

56 A. Habenschuss and F. H. Spedding, *J. Chem. Phys.*, 1979, **70**, 2797.
57 A. Habenschuss and F. H. Spedding, *J. Chem. Phys.*, 1980, **71**, 442.
58 C. Cossy, L. Helm, D. H. Powell and A. E. Merbach, *New J. Chem.*, 1995, **19**, 27.
59 L. Helm and A. E. Merbach, *Eur. J. Solid State Inorg. Chem.*, 1991, **28**, 245.
60 B. K. Annis, R. L. Hahn and A. H. Narten, *J. Phys. Chem.*, 1985, **82**, 2086.
61 T. Yaita, H. Narita, S. Suzuki, S. Tachimori, H. Motohashi and H. Shiwaku, *J. Radioanal. Nucl. Chem.*, 1999, **239**, 371.
62 T. Yamaguchi, M. Nomura, H. Wakita and H. Ohtaki, *J. Chem. Phys.*, 1988, **89**, 5153.
63 F. David and C. den Auwer, unpublished results.
64 C. Cossy, A. C. Barnes, J. E. Enderby and A. E. Merbach, *J. Chem. Phys.*, 1989, **90**, 3254.
65 E. N. Rizkalla and G. R. Choppin, in *Handbook on the Physics and Chemistry of Rare Earths. Lanthanides/Actinides: Chemistry*, ed. K. A. Gschneider, L. Eyring, G. R. Choppin and G. H. Lander, Elsevier Science, Amsterdam, pp. 529–558, 1994.
66 R. D. Shannon, *Acta Crystallogr.*, *Sect. A*, 1976, **32**, 751.
67 As a matter of comparison with previously published parameters, we simulated Eu^{3+} with the parameters of Auffinger *et al.*[22] and Gd^{3+} with those of Fossheim *et al.*[25–27] and of Judson *et al.*[29] They were less satisfactory than ours, as the resulting M–Ow distances were either somewhat too short (2.23 Å for Eu^{3+}) or too long (2.53 and 2.58 Å for Gd^{3+}) compared to experiment (Eu–Ow = 2.43[63]–2.45 Å[55–57] and Gd–Ow = 2.41[62,63]–2.42 Å[61]). The corresponding calculated CN's were also either slightly lower (8.1 ± 0.01) or larger (9.2 ± 0.01 or 10.0 ± 0.01) than experimental CN's which are between 8.3[55–57] and 8.6[61,62] for Eu^{3+} and between 7.6[62] and 8.0[61] for Gd^{3+}. One also notes that the van Veggel *et al.*[36] parameters satisfactorily reproduce free energies of hydration of lanthanides and cation–water distances, but seem to overestimate the CN's (from 10 to 9 across the lanthanide series). Our parameters are therefore satisfactory from the energy and structural points of view for aqua ions.
68 D. Matkovic-Calogovic, *Acta Crystallogr.*, *Sect. C*, 1988, **44**, 435.
69 Changes in solvent–solvent interaction energies also contribute to the preferred stabilities. However, the latter can hardly be compared, as the number of solvent molecules is not identical for the two simulated systems, and their energies display large statistical fluctuations. In addition, entropy effects, not amenable to simple evaluation from the MD trajectories, also contribute to the nature of the complex.
70 N. Muzet, G. Wipff, A. Casnati, L. Domiano, R. Ungaro and F. Ugozzoli, *J. Chem. Soc.*, *Perkin Trans. 2*, 1996, 1065.
71 F. Berny, N. Muzet, L. Troxler, A. Dedieu and G. Wipff, *Inorg. Chem.*, 1999, **38**, 1244.
72 C. Boehme and G. Wipff, *Inorg. Chem.*, 1999, **38**, 5734.

Paper a908879b